Loss of VHL and Hypoxia Provokes PAX2 Up-Regulation in Clear Cell Renal Cell Carcinoma

Van-Duc Luu,[1] Gunther Boysen,[1] Kirsten Struckmann,[1] Silvia Casagrande,[1] Adriana von Teichman,[1] Peter J. Wild,[1] Tullio Sulser,[2] Peter Schraml,[1] and Holger Moch[1]

Abstract

Purpose: The paired box gene 2, PAX2, encodes for a transcription factor that is up-regulated during nephrogenesis and becomes silenced in mature epithelium of the glomeruli, the proximal, and distal tubules. Reactivation of PAX2 has been frequently observed in clear cell renal cell carcinoma (ccRCC), a tumor type characterized by loss of von Hippel-Lindau (VHL) tumor suppressor function. The regulation of PAX2 expression in ccRCC is unknown.

Experimental Design: We applied reporter gene assays to investigate PAX2 promoter regulation. Furthermore, PAX2 expression was determined in ccRCC cell lines under normoxic and hypoxic condition in a VHL wild-type and mutated background. PAX2 expression was also assessed in 831 human ccRCC and correlated with hypoxia-inducible factor α (HIFα) and clinical parameters.

Results: Here, we show that both loss of VHL protein (pVHL) function and hypoxia leads to strong PAX2 reexpression. Using luciferase reporter gene assays, no induction was obtained in spite of six hypoxia response element motifs identified in the promoter of PAX2. Comprehensive immunohistochemical analyses showed significant correlations between PAX2, HIF1α, and HIF2α—target CCND1 expression patterns in ccRCC patients. Notably, PAX2 expression was highly associated with early-stage, well-differentiated ccRCC and, consequently, better clinical outcome ($P < 0.0001$ each). Additional analyses indicated that PAX2 repressor WT1 and cancer-linked hypomethylation are not important for transcriptional regulation of PAX2 in ccRCC.

Conclusion: We conclude that in ccRCC, PAX2 reactivation is driven by HIF-dependent mechanisms following pVHL loss.

The majority of sporadic clear cell renal cell carcinoma (ccRCC) is characterized by von Hippel-Lindau (*VHL*) gene mutations that dysregulate the function of the VHL protein (pVHL; ref. 1). pVHL acts as a multipurpose adaptor protein, which is part of distinct multiprotein complexes controlling microtubule-based processes, extracellular matrix assembly, and transcription regulatory pathways (2). The best-described function of pVHL as transcriptional regulator is its ability of targeting the α subunits of HIF for ubiquitin-mediated proteolysis via E3 ubiquitin protein ligase complex (3, 4). In ccRCC, loss of pVHL function provokes cell invasion, angiogenesis, glucose metabolism, and survival but also destabilization of microtubules and primary cilia (5–9). An essential part of these processes is evoked by HIF-mediated gene expression programs. Stabilization of HIF due to VHL mutation considerably contributes to both ccRCC formation and progression.

More than 100 putative HIF target genes either indirectly activated or directly regulated by a functional HIF binding site have been identified (10). Common and contrasting properties of the functions of the two isoforms HIF1α and HIF2α have been described in different cancer cell types (11, 12). Interestingly, HIFα isoforms displayed suppressive interactions in RCC cells, with enhanced expression of HIF2α suppressing HIF1α and vice versa (11). Although binding the same DNA motif, it is yet unclear how HIF1α and HIF2α are able to differently regulate common and unique target genes. The identification of additional yet unknown HIF target genes would contribute to a better understanding of the common and different roles of HIF1α and HIF2α in ccRCC.

Authors' Affiliations: [1]Department of Pathology, Institute of Surgical Pathology and [2]Department of Urology, University Hospital Zurich, Zurich, Switzerland

Received 10/24/08; revised 1/15/09; accepted 2/8/09; published OnlineFirst 4/28/09.

Grant support: UBS AG (made possible by an anonymous donor), Swiss National Science Foundation (3238BO-103145), and Zurich Cancer League, Switzerland.

The costs of publication of this article were defrayed in part by the payment of page charges. This article must therefore be hereby marked *advertisement* in accordance with 18 U.S.C. Section 1734 solely to indicate this fact.

Note: Supplementary data for this article are available at Clinical Cancer Research Online (http://clincancerres.aacrjournals.org/).

V-D. Luu and G. Boysen contributed equally to this work. P. Schraml and H. Moch shared senior authorship.

Requests for reprints: Holger Moch, Department of Pathology, Institute of Surgical Pathology, University Hospital Zurich, Zurich 8091, Switzerland. Phone: 41-44-2552510; Fax: 41-44-2554440; E-mail: holger.moch@usz.ch.

doi:10.1158/1078-0432.CCR-08-2779

Translational Relevance

In clear cell renal cell carcinoma (ccRCC), the activation of hypoxia-inducible factor α (HIFα)–mediated transcriptional programs is caused by loss of function of the von Hippel-Lindau protein (pVHL). The identification of yet unknown HIF target genes will improve our understanding of the biological consequences of a deregulated VHL/HIF pathway in ccRCC, a prerequisite for the development of therapeutic anticancer strategies. The transcription factor *PAX2* has been recently suggested as a potential therapeutic target gene in renal cancer. We have found that PAX2 is negatively regulated by pVHL and is induced by hypoxia. Furthermore, we observed a significant correlation between PAX2 and HIFα in ccRCC patients. Notably, PAX2 expression correlated with tumor grade and stage in ccRCC. This is the first study showing HIF-dependent up-regulation of the cancer target gene *PAX2* as a consequence of VHL loss of function in ccRCC cell lines and human tumor tissues.

The paired box gene 2, also termed *PAX2*, is a member of the *PAX* gene family of developmental transcription factors that is abundantly expressed in the developing eyes, ears, central nervous, and urogenital systems (13). Induction of nephrogenesis by the ureter is accompanied by up-regulation of PAX2 followed by cell proliferation of the ureteric bud and transactivation of the promoter of the tumor suppressor gene *WT1*, which leads to repression of PAX2 and the differentiation of the nephrogenic mesenchyme (14). In addition to fetal tissues, high levels of PAX2 expression were also observed in several human tumors, including leukemia; breast, ovarian, endometrium, and prostate cancer; Wilms' tumor; as well as ccRCC (15).

Little is known about the regulatory mechanisms leading to the activation of PAX2 expression in ccRCC. Two transcription start sites within the *PAX2* promoter have been reported in a Wilms' tumor sample (16). In endometrial carcinoma, PAX2 was shown to be activated by hypomethylation of its promoter in an estrogen- and tamoxifen-dependent manner (17). Our sequence analysis of the *PAX2* promoter region revealed six putative hypoxia response elements (HRE). As PAX2 is absent in normal renal tubular epithelial cells but expressed in 88% to 100% of ccRCC (18–20), the up-regulation of PAX2 might be caused by either cancer-linked hypomethylation or HIF stabilization as a consequence of pVHL loss of function. In this study, we investigated both the methylation status of the *PAX2* promoter and the regulatory role of HIF for PAX2 expression in ccRCC.

Materials and Methods

Analysis of the PAX2 promoter. Computer-assisted *PAX2* promoter analysis was done using Genomatix Gene2Promoter software[3] and EMBL sequence AF515729 to identify potential HREs. CpG islands were detected using the CpG Island Searcher program.[4]

[3] http://www.genomatix.de
[4] http://www.cpgislands.com

Methylation-specific PCR. In total, 20 frozen ccRCC tissue samples and their corresponding normal kidney samples were analyzed. Genomic DNA was extracted using Qiagen Blood and Tissue kit and bisulfite converted using EZ DNA Methylation kit (Zymo Research). The same methylation-specific primers for the *PAX2* promoter were used as published by Wu et al. (17). DNA from a subset of patients treated with *Sss*I methyltransferase (New England Biolabs) was used as a positive control for methylated alleles.

Cell culture. The ccRCC-derived cell line 786-O and the human embryonic kidney cell line HEK-293 were supplied by the American Type Culture Collection. Stable transfectant of 786-O reexpressing $pVHL_{30}$ was generated as mentioned (21). The RCC4 cell line and its corresponding transfectant RCC4 VHL reexpressing wild-type $pVHL_{30}$ were created as described (5, 7). Human renal proximal tubular epithelial cell line HK-2 was provided by R. Wüthrich (Clinic for Nephrology, Department of Internal Medicine, University Hospital Zurich, Zurich, Switzerland). RCC4, HEK-293, and HK-2 were cultured as reported previously (22). Hypoxic experiments with HK-2 and RCC4 were done for 16 h at 1% oxygen using an Invivo2 400 hypoxia workstation (Biotrace International). Dimethyloxallyl glycine (DMOG; Cayman Chemical) treatment in HK-2 and HEK-293 cells was done at 1 mmol/L over 24 h. Cobalt chloride ($CoCl_2$; Sigma) treatment in 786-O and 786-O $pVHL_{30}$ was done at 0.5 mmol/L over 24 h.

HIF2α short hairpin RNA constructs and lentiviral infections. Expression vectors encoding short hairpin RNA sequences targeting human HIF2α were purchased from Sigma (shHIF2α #1, clone ID NM_001430.x-517s1c1 and shHIF2α #4, clone ID NM_001430.x-1694s1c1, respectively). Viral particles were produced using ViraPower lentiviral expression system according to the manufacturer's instructions (Invitrogen). Briefly, 786-O and 786-O $pVHL_{30}$ cells were infected with lentiviral particles of either shHIF2α #1 or shHIF2α #4 constructs and pool of clones was derived by puromycin selection (4 μg/mL). Pools of clones were analyzed for effective HIF2α knockdown by quantitative reverse transcription-PCR and anti-HIF2α immunoblotting.

Tissue specimen and tissue microarray construction. We used tissue microarrays (TMA) comprising 831 nephrectomy ccRCC collected from the University Hospital Zurich, the Kantonsspital St. Gallen (St. Gallen, Switzerland), and the University Hospital of Basel (Basel, Switzerland). All ccRCC samples were histologically reviewed by one pathologist (H.M.) and selected for the study based on H&E-stained tissue sections. For all cohorts, a RCC TMA was constructed as previously described (23). This study was approved by the local commission of ethics (reference number StV 38-2005). Clinical information was obtained for 519 cases. The mean age of patients was 62.7 (15-88) and mean follow-up was 51.9 mo (0.1-229). Tumors were graded according to the Thoenes grading system and histologically classified according to the WHO classification (24). There were 163 grade 1 (20%), 415 grade 2 (50%), 248 grade 3 (30%), 161 pT1 (20%), 223 pT2 (27%), 412 pT3 (50.5%), and 20 pT4 (2.5%) tumors.

Western blot analysis. Whole-cell lysates were prepared using radioimmunoprecipitation assay buffer (Sigma) containing complete protease inhibitor cocktail (Roche). Homogenization was done with a tissue lyser (Qiagen) for 4 min at 20 Hz. Lysates were centrifuged for 10 min (2,500 × *g*, 4°C). Protein concentration of the supernatant was determined by the bicinchoninic acid assay (Pierce) with bovine serum albumin as a standard. Equivalent amounts of protein (15-50 μg) were separated on NuPAGE Bis-Tris Gels with a gradient of 4% to 12% (Invitrogen) and transferred to nitrocellulose membranes (Schleicher/Schuell). Membranes were blocked in TBS-Tween 20 containing 5% (w/v) nonfat dry milk for 1 h at room temperature. After washing in TBS-Tween 20, membranes were incubated overnight at 4°C using the following primary antibodies: rabbit polyclonal anti-PAX2 (clone C-RX2; 1:1,000; Invitrogen), rabbit polyclonal anti-HIF2α (clone NB100-122; 1:1,000; Novus Biologicals), mouse monoclonal lamin A/C (1:3,000; BD Biosciences), and mouse monoclonal anti–β-actin (clone MAB1501; 1:10,000; Chemicon International). After washing with TBS-Tween 20, the membranes were incubated at room temperature with

horseradish peroxidase–conjugated secondary antibody rabbit anti-mouse (1:3,000; Dako) or goat anti-rabbit (1:3,000; Dako). The protein-antibody complexes were detected by enhanced chemiluminescence (Amersham).

Reporter gene assay. The *PAX2* promoter (16) was obtained by PCR amplification of genomic DNA using the oligonucleotide primers 5′-ATGCACTAGTCCTGCAGGAGGAGGAGAGG-3′ and 5′-ATGCGATATCCTCCCGGTGTGTGTCTCTCT-3′. PCR products were sequenced using the ABI Prism 3100 Genetic analyzer (Applied Biosystems). pGLPAX2prom was constructed by insertion of a 3.47-kb *Spe*I-*Eco*RV fragment from the human *PAX2* promoter into the *Nhe*I-*Eco*RV sites of a pGL4.10 firefly luciferase reporter plasmid (Promega). For transcriptional transactivation experiments, HEK-293 and HK-2 cells were transfected with 1 μg of pGLPAX2prom reporter plasmid along with 100 ng of pGL4.74 *Renilla* luciferase reporter plasmid (Promega) in 24-well plates using FuGene 6 reagent (Roche Molecular Biochemicals). pGl3P2P(607bp) vectors are 5′-truncated versions of the previously published pGl3b(1454/3172)P2P plasmids containing the wild-type or mutated HRE of the human PHD2 promoter (provided by Dr. Daniel Stiehl, University of Zurich, Zurich, Switzerland). pGLTf are pGL3prom vectors (Promega) that carry either wild-type HRE (HREww) or antisense sequence (ERHmm) derived from transferrin enhancer (25). These vectors served as positive and negative controls for HIFα activity. After transfection, cells were incubated with and without DMOG (1 mmol/L) for 24 h. Luciferase activity was measured after cell lysis using the dual-luciferase reporter assay system (Promega). Relative luciferase units were determined by dividing the luciferase activity of the pGL4.10 reporter constructs by that of the pGL4.74 control reporter.

Immunohistochemistry. TMA sections (2.5 μm) were transferred to glass slides followed by immunohistochemical analysis according to the Ventana automat protocols. The same antibodies used for Western blot analysis were applied for detection of PAX2 (dilution, 1:500), HIF1α (1:500; Abcam Ltd.), CCND1 (clone SP4, 1:40; Labvision), and WT1 (clone 6F-H2, 1:50; Dako). Analysis was done with a Leitz Aristoplan microscope (Leica). Pictures of ccRCC specimens were taken with the digital camera KY-070 (JVC). Tumors were considered PAX2, HIF1α, CCND1, or WT1 positive if >5% of tumor cells showed nuclear expression. All TMAs were analyzed by one pathologist (P.J.W.).

Statistical analysis. Contingency table analysis, χ^2 tests, Kaplan-Meier curve, and log-rank tests for evaluating correlations between PAX2, HIF1α, and CCND1 expression as well as clinical parameters were calculated using StatView 5.0 (SAS).

Results

HRE sequences and CpG islands in the* PAX2 *promoter. Our *in silico* sequence analyses revealed six potential HREs

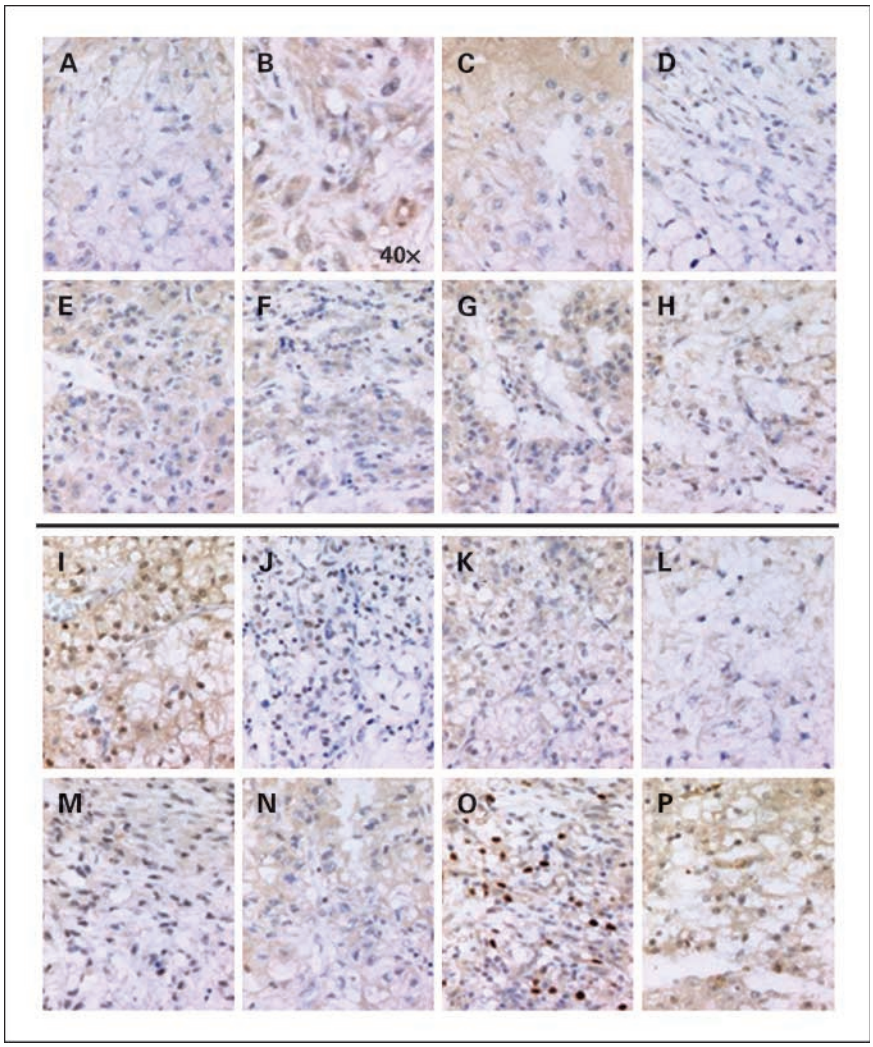

Fig. 1. PAX2 expression pattern in 16 sporadic ccRCC patients. *A* to *H*, tumors with wild-type *VHL*. *I* to *P*, tumors with mutated *VHL*.

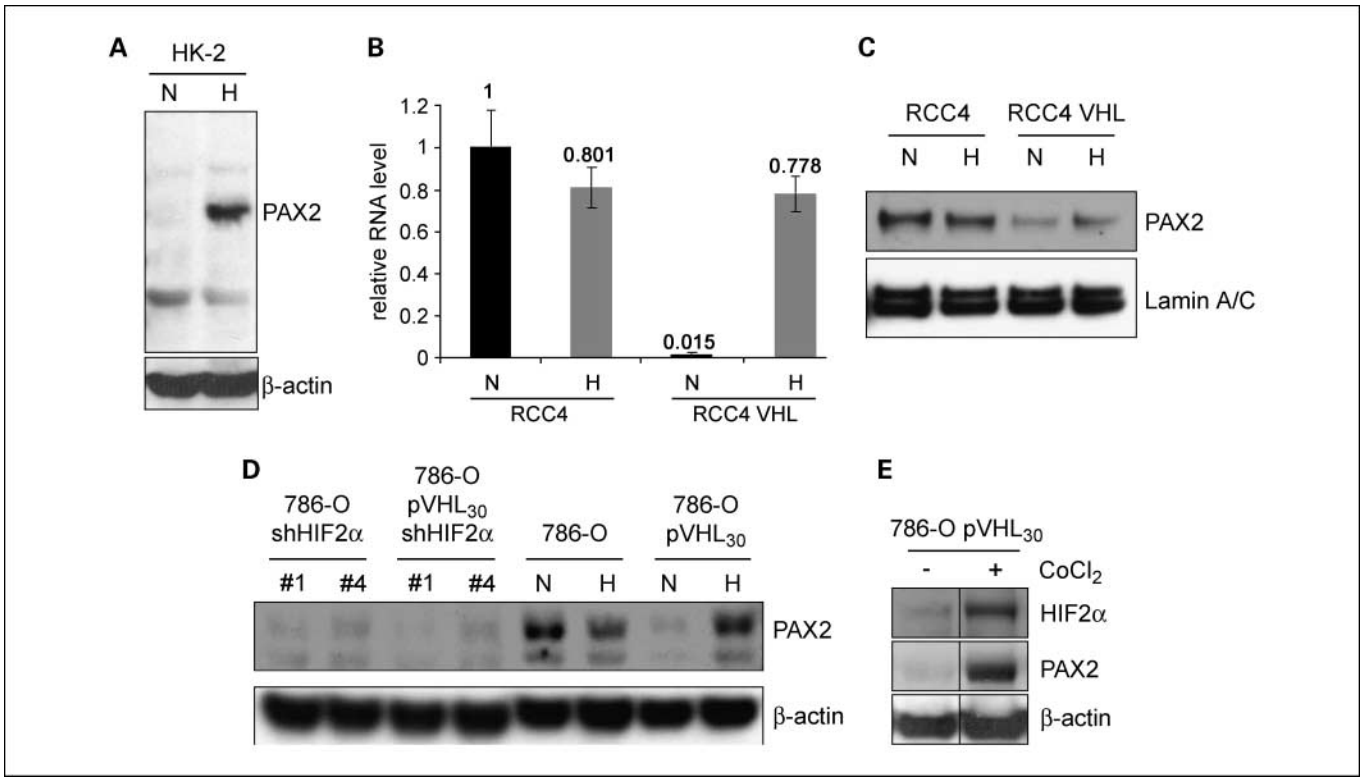

Fig. 2. *A,* Western blot analysis of HK-2 cells grown under normoxia (*N*) and hypoxia (*H*). β-Actin was used as a loading control. *B,* relative *PAX2* mRNA expression level of RCC4 and RCC4 VHL cells under normoxic and hypoxic conditions as measured by quantitative real-time PCR. Transcript level at normoxia was set to 1. Columns, mean of three independent experiments; bars, SE. *C,* PAX2 protein expression in RCC4 and RCC4 VHL cells under normoxia and hypoxia. *D,* PAX2 protein level in the ccRCC-derived cell lines 786-O and 786-O $pVHL_{30}$ under normoxia and hypoxia and with silenced HIF2α background. Lamin A/C was used as loading control. *E,* PAX2 protein level in 786-O $pVHL_{30}$ subjected to $CoCl_2$ treatment.

(gcgtg) in the 3,476-bp *PAX2* promoter region (3,810-3,806, 2,536-2,532, 1,996-1,992, 1,801-1,797, 1,387-1,383, and 1,312-1,308 bp 5′ of the ATG start codon; see Supplementary Fig. S1A for details). We also detected three putative CpG islands with a minimal length of 100 bp in the 4,158-bp region (promoter and 5′-untranslated region) upstream of the ATG start codon (Supplementary Fig. S1B).

PAX2 expression in VHL mutated and wild-type ccRCC. The presence of several HRE motifs in the *PAX2* promoter region prompted us to investigate whether PAX2 expression is HIF dependent and regulated by pVHL in ccRCC. Here, we used a small TMA consisting of 16 ccRCC (8 with wild-type *VHL* and 8 with *VHL* frameshift mutations). PAX2 was expressed only weakly in two wild-type *VHL* patients, whereas moderate and strong nuclear PAX2 staining was seen in six of eight VHL mutated ccRCC (Fig. 1).

PAX2 expression under hypoxia. To test whether PAX2 expression is HIF dependent, VHL-positive renal proximal tubular cells HK-2 were subjected to hypoxia. HK-2 cells do not express PAX2 at normoxic condition. PAX2 protein level was strongly up-regulated after 16 hours of hypoxia, suggesting a HIF-dependent induction of PAX2 (Fig. 2A).

PAX2 expression under hypoxia in VHL-positive and VHL-negative tumor cells. We investigated whether the up-regulation of PAX2 levels under hypoxic conditions is VHL dependent. To this end, we used the ccRCC cell line RCC4 and its corresponding transfectant RCC4 VHL reexpressing wild-type $pVHL_{30}$. Figure 2B shows the *PAX2* transcript levels in RCC4 and RCC4 VHL grown under normoxic and hypoxic conditions. The *PAX2* transcript level remains stable under hypoxia in RCC4 cells. In RCC4 VHL, *PAX2* was drastically reduced under normoxia, whereas hypoxia led to a 52-fold increase of the *PAX2* level (Fig. 2B), which is comparable with that of RCC4 cells under hypoxic condition. The *PAX2* mRNA expression data could further be confirmed with immunoblotting data (Fig. 2C), although induction of PAX2 expression under hypoxia in RCC4 VHL cells is somewhat weaker than observed on the mRNA level. We also determined the PAX2 expression level in 786-O and 786-O $pVHL_{30}$ cell lines. Here, we observed a higher PAX2 level in 786-O cells compared with 786-O $pVHL_{30}$ under normoxic condition (Fig. 2C). Similar to RCC4 VHL cells, an increase of PAX2 level was observed under hypoxia in 786-O $pVHL_{30}$ cells (Fig. 2C). This expression was comparable with that of VHL-negative 786-O cells, suggesting again a role for pVHL in regulating PAX2 expression via HIF. In addition, silencing of HIF2α by RNA interference leads to a reduction of PAX2 in these cell lines (Fig. 2D). To further evaluate whether the VHL/HIF signaling pathway is involved in PAX2 regulation, 786-O $pVHL_{30}$ cells were treated with $CoCl_2$, which resulted in an up-regulation of both HIF2α and PAX2 (Fig. 2E), again confirming HIF-dependent regulation of PAX2.

PAX2 promoter reporter gene assays. Luciferase reporter assays were done to verify the functionality of the putative HREs in the promoter region of *PAX2*. For this purpose, a *PAX2* promoter DNA fragment was inserted upstream of a promoterless luciferase reporter gene vector. Following transient transfection, HEK-293 cells were treated with and without DMOG. DMOG is a prolyl hydroxylase inhibitor resulting in HIFα stabilization

and increased HIF activity. The reporter activity of the vector containing the whole *PAX2* promoter was unchanged in HEK-293 cells after treatment with DMOG compared with untreated cells (Fig. 3A). Specificity of DMOG-induced HIF activity was shown by using reporter vectors comprising wild-type or mutated HREs of the HIF target prolyl hydroxylase 2 (P2P). A 2.6-fold induction of the P2P wild-type reporter indicated the activation of the HIF pathway after DMOG treatment. No increase of luciferase activity was measured in the vector containing the mutated HRE of P2P (Fig. 3A). Similar experiments were done for HK-2 cells. Here, the integrity of the luciferase reporter gene assay was tested by measuring the activity of wild-type and mutated transferrin promoter pGLTfHREww and pGLTfERHmm, respectively. *PAX2* promoter (pGLPAX2prom) activity remained unchanged on DMOG treatment in HK-2 cells (Fig. 3B). These results show that the identified putative HRE in the *PAX2* promoter region is not sufficient for the induction of PAX2 expression by HIF in HEK-293 and HK-2 cells.

Correlation of PAX2 expression with HIF1α and HIF2α expression in ccRCC tissues. The results from the *in vitro* experiments motivated us to further investigate PAX2 expression in relation to HIF expression. To this end, we analyzed TMAs comprising 831 ccRCC to evaluate the correlation between PAX2 and HIF1α expression. Of 294 PAX2-positive tumors, 222 (75.5%) also expressed HIF1α ($P < 0.0001$). Due to technical problems with HIF2α antibody on immunohistochemistry, we used the HIF2α target CCND1 as readout for HIF2α. Of 310 PAX2-expressing tumors, 253 (81.6%) stained also positive for CCND1 ($P < 0.0001$).

Correlation between PAX2 expression and tumor grade, stage, and survival. We next investigated the relations of PAX2 expression to clinicopathologic parameters in ccRCC. We observed a strong differentiation grade-dependent PAX2 expression in ccRCC. One hundred three of 155 (66.5%) grade 1 tumors expressed PAX2, whereas in grade 3 tumors 54 of 228 (23.7%) were PAX2 positive (Table 1). We also observed decreasing PAX2 expression with increasing tumor stage. For example, only 2.7% of pT3 and pT4 tumors show strong PAX2 staining intensity (Table 1). Consequently, there was also a significant correlation between PAX2 level and overall survival in ccRCC patients (Fig. 4). Patients with PAX2 expression had a better prognosis than patients with PAX2-negative tumors. However, the association between PAX2 expression and clinical outcome was not independent from tumor grade and tumor stage (data not shown).

PAX2 expression in ccRCC is not dependent on hypomethylation. Several ccRCC (24.5%) showed no correlation between PAX2 and HIF1α expression, suggesting other mechanisms for PAX2 up-regulation in these cancers. The existence of CpG islands in the promoter region of *PAX2* led us to investigate whether PAX2 expression in ccRCC might be controlled by epigenetic mechanisms. We assessed the methylation status of *PAX2* promoter by methylation-specific PCR. In total, we analyzed 20 ccRCC and their patient-matched normal kidney tissue. In all normal and tumor samples, *PAX2* promoter was unmethylated (examples are shown in Fig. 5A). *In vitro* methylated DNA from a patient subset served as a positive control for methylated alleles (Fig. 5B).

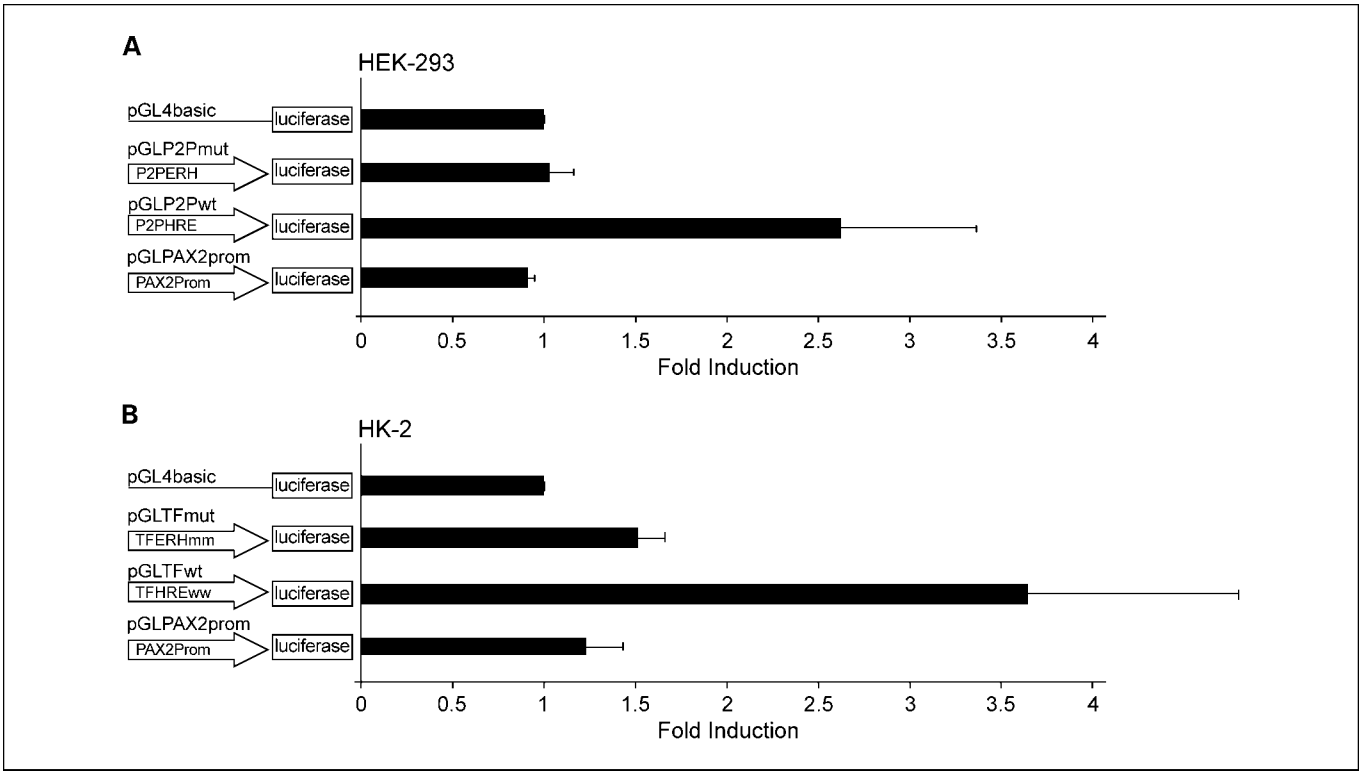

Fig. 3. HIF responsiveness of the *PAX2* promoter region. Luciferase reporter gene activity following transient transfection with or without HIF induction by DMOG for 24 h of HEK-293 (*A*) and HK-2 (*B*) cells with luciferase expression plasmids containing the 3.5-kb *PAX2* promoter. A cotransfected *Renilla* luciferase expression vector served as internal control for transfection efficiency. Fold induction is relative to reporter gene activities of HEK-293 cells without DMOG treatment. Positive and negative controls are described in Materials and Methods. Columns, mean; bars, SD.

Table 1. Correlation between PAX2 expression and tumor grade and stage

Tumor	PAX2 intensity, *n* (%)					PAX2-expressing cells, *n* (%)			
	Negative	Weak	Moderate	Strong	*P*	0-5%	6-50%	>50%	*P*
Grade 1	52 (33.5)	44 (28.4)	20 (12.9)	39 (25.2)	<0.001	52 (33.5)	18 (11.6)	85 (54.8)	<0.001
Grade 2	233 (59.4)	102 (26.0)	40 (10.2)	17 (4.3)		233 (59.4)	46 (11.7)	113 (28.8)	
Grade 3	174 (76.3)	36 (15.8)	12 (5.3)	6 (2.6)		174 (76.3)	16 (7.0)	38 (16.7)	
pT1,2	178 (49.4)	93 (25.8)	40 (11.1)	49 (13.6)	<0.001	178 (49.4)	38 (10.6)	144 (40.0)	<0.001
pT3,4	278 (68.5)	86 (21.2)	31 (7.6)	11 (2.7)		278 (68.5)	41 (10.1)	87 (21.4)	

NOTE: Please note combined pT stages (pT1,2 and pT3,4).

Discussion

In this study, we investigated the molecular mechanisms leading to PAX2 up-regulation in ccRCC. Detailed sequence analysis of the *PAX2* promoter unmasked HREs and CpG islands, suggesting that the up-regulation of PAX2 in ccRCC is driven by HIF and/or cancer-linked hypomethylation. Our *in vitro* analysis revealed that in ccRCC, the activation of transcription regulator PAX2 is induced by hypoxia and depends on the functional integrity of pVHL. An additional TMA-based analysis of 831 ccRCC showed that PAX2 is preferentially expressed in highly differentiated early-stage tumors. PAX2 expression was significantly correlated with the expression of HIF1α and HIF2α target CCND1, indicating that PAX2 activation is mainly regulated by HIF.

The identification of six putative HRE consensus sequences in the *PAX2* promoter prompted us to analyze PAX2 expression in pVHL-negative and pVHL-transfected RCC4 cells and normal pVHL-positive HK-2 and HEK-293 cells. Up-regulation of PAX2 was seen in RCC4 but not in pVHL-positive transfectant and HK-2. Increased expression of PAX2 was determined in DMOG-treated HK-2 cells and pVHL-expressing RCC4. In wild-type RCC4, PAX2 protein expression levels remained stable under normoxia and hypoxia. Luciferase reporter gene assays were applied to confirm the HIF-induced activation of the *PAX2* promoter. These experiments failed to show an increased activity of a reporter vector containing the *PAX2* promoter after stabilization of HIF. Therefore, our *in vitro* data imply molecular mechanisms for PAX2 expression in ccRCC, which necessitate other tissue-specific factors in addition to HIF. Given the nature of HRE as an enhancer, it might also be possible that relevant HREs outside the *PAX2* promoter are responsible for HIF induction. HIF-independent activation of genes under hypoxia has been described, for example, for mammalian target of rapamycin (26) and DNASE1 (27). Transcriptional response to PAX2 might also be mediated by yet unknown *cis*-acting elements located outside the *PAX2* promoter. Such enhancer elements have been identified 3′ to the human erythropoietin gene (28).

We further confirmed our *in vitro* results that showed the influence of pVHL on PAX2 expression by using a small TMA with arrayed normal renal tissues, VHL wild-type ccRCC, and ccRCC with frameshift mutations (1, 29). As expected, all normal tissues were PAX2 negative, whereas only 2 of 8 VHL wild-type ccRCC but 6 of 8 (75%) VHL mutated tumors expressed PAX2. PAX2 expression correlated with the presence of *VHL* "loss-of-function" mutations (1, 29), which highly likely cause pVHL loss and stabilize HIF.

PAX2 expression has previously been described in ccRCC cell lines and tissues (18–20, 30). In these studies, relative small numbers of ccRCC were analyzed and the frequencies of PAX2-positive tumors varied between 88% and 100%. We significantly extended these studies using TMAs that contained 831 ccRCC specimens. Here, we showed that PAX2 was expressed predominantly in early-stage and low-grade cancers. This observation suggests that the up-regulation of PAX2 represents an early step in ccRCC development. To test whether PAX2 activation is dependent on HIF, we analyzed the expression of HIF1α and HIF2α target CCND1 on our ccRCC TMAs. The significant correlation between PAX2, HIF1α, and CCND1 expression strongly argues for a direct or indirect regulatory effect of both HIF1α and HIF2α on PAX2 transcription.

The ability to transcriptionally repress the tumor suppressor p53 (31) and its joint action with CCND1 makes PAX2 an important promoter of cell proliferation, which might be regarded as one of the most critical steps toward ccRCC development. In humans with kidney malformations, including polycystic kidney disease and juvenile cystic kidneys, it was shown that PAX2 is abundantly present in cystic and hyperproliferative epithelial cells (32, 33). Reduced *PAX2* gene dosage inhibited significantly renal cyst growth in mice (34). Interestingly, patients with hereditary and sporadic ccRCC also frequently have intratumoral cysts (35), which are thought to be a result of uncontrolled cell proliferation and represent tumor precursor lesions

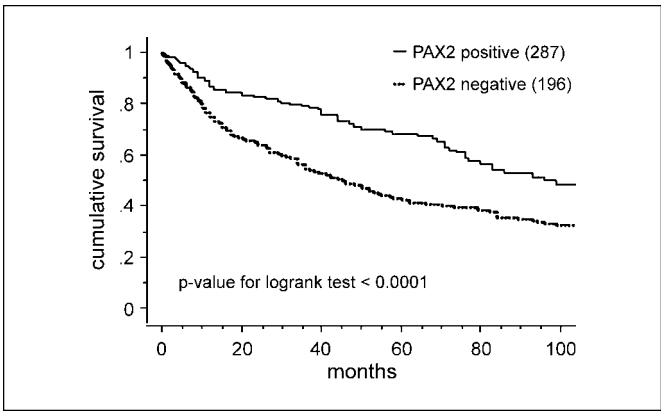

Fig. 4. PAX2 expression and overall survival in ccRCC patients.

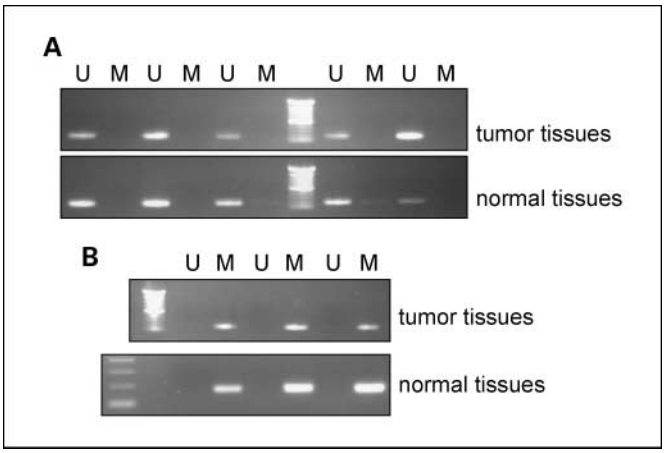

Fig. 5. *A,* methylation-specific PCR analysis detecting methylation status of *PAX2* promoter in ccRCC and normal patient-matched kidney tissues. U, unmethylated *PAX2*; M, hypermethylated *PAX2* promoter. *B, in vitro* methylated DNA as control for methylated *PAX2* alleles.

(36, 37). It is therefore tempting to speculate that PAX2 is the driving force for cyst formation in ccRCC.

As PAX2 is silenced in normal renal tubular epithelial cells, reactivated in early ccRCC stage, and down-regulated during tumor progression, it seems obvious that HIF is not the only factor being responsible for PAX2 expression. Our finding that PAX2 and HIF positivity was not correlated in 24.5% of the tumors suggests other molecular factors that regulate PAX2 transcription. We therefore looked for additional possible mechanisms that would explain at least in part the discrepant PAX2 expression patterns. As it was shown in endometrial cancer, activation of PAX2 is associated with hypomethylation of its promoter (17). Using the same protocols, hypermethylation of *PAX2* promoter was seen neither in normal renal tissue nor in late-stage ccRCC, suggesting that the transcriptional regulation of PAX2 differs between endometrial cancer and ccRCC.

Previous studies showed that PAX2 is repressed by WT1 during normal kidney development (14) and that PAX2 is up-regulated in Wilms' tumor (38). Because the frequencies reported for WT1 expression in RCC are rather inconsistent (39–41), we compared WT1 and PAX2 expression on our TMAs. None of the normal renal tissues and only 5% of the ccRCC stained weakly for WT1, excluding a key role of WT1 as transcriptional repressor of PAX2 in ccRCC (data not shown). Considerable genetic heterogeneity between primary RCC and metastases has been previously described and suggests the existence of yet unknown genetic factors contributing to PAX2 down-regulation during the metastatic process.

In summary, our *in vitro* and *in vivo* data show that in ccRCC *PAX2* is a hypoxia-regulated gene negatively controlled by pVHL. The frequent expression of PAX2 in ccRCC and its highly significant correlation with better clinical outcome together with its oncogenic function might validate PAX2 as appropriate target for renal cancer therapy. In normal kidney cells and fetal kidney explants, PAX2 conferred resistance to cisplatin-induced apoptosis (42). Xenografts of shPAX2-treated ACHN cell line in nude mice confirmed that the tumors were more responsive to cisplatin therapy than PAX2-positive control cells. These results might implicate PAX2 as potential predictive marker in ccRCC, especially for those patients with organ-confined ccRCC that will develop metastasis and succumb to their disease.

Disclosure of Potential Conflicts of Interest

No potential conflicts of interest were disclosed.

Acknowledgments

We thank Martina Storz, Susanne Dettwiler, and Silvia Behnke for their excellent technical support and Dr. Daniel Stiehl for his helpful advice and suggestions.

References

1. Banks RE, Tirukonda P, Taylor C, et al. Genetic and epigenetic analysis of von Hippel-Lindau (VHL) gene alterations and relationship with clinical variables in sporadic renal cancer. Cancer Res 2006;66:2000–11.
2. Frew IJ, Krek W. Multitasking by pVHL in tumour suppression. Curr Opin Cell Biol 2007; 19:685.
3. Maxwell PH, Wiesener MS, Chang GW, et al. The tumour suppressor protein VHL targets hypoxia-inducible factors for oxygen-dependent proteolysis [see comments]. Nature 1999;399: 271–5.
4. Ohh M, Park CW, Ivan M, et al. Ubiquitination of hypoxia-inducible factor requires direct binding to the β-domain of the von Hippel-Lindau protein. Nat Cell Biol 2000;2:423–7.
5. Hergovich A, Lisztwan J, Thoma CR, Wirbelauer C, Barry RE, Krek W. Priming-dependent phosphorylation and regulation of the tumor suppressor pVHL by glycogen synthase kinase 3. Mol Cell Biol 2006;26:5784–96.
6. Barry RE, Krek W. The von Hippel-Lindau tumour suppressor: a multi-faceted inhibitor of tumourigenesis. Trends Mol Med 2004;10:466.
7. Hergovich A, Lisztwan J, Barry R, Ballschmieter P, Krek W. Regulation of microtubule stability by the von Hippel-Lindau tumour suppressor protein pVHL. Nat Cell Biol 2003;5:64.
8. Thoma CR, Frew IJ, Hoerner CR, Montani M, Moch H, Krek W. pVHL and GSK3β are components of a primary cilium-maintenance signalling network. Nat Cell Biol 2007;9:588–95, Epub 2007 Apr 22.
9. Frew IJ, Krek W. pVHL: a multipurpose adaptor protein. Sci Signal 2008;1:e30.
10. Wenger RH, Stiehl DP, Camenisch G. Integration of oxygen signaling at the consensus HRE. Sci STKE 2005;2005:re12.
11. Raval RR, Lau KW, Tran MG, et al. Contrasting properties of hypoxia-inducible factor 1 (HIF-1) and HIF-2 in von Hippel-Lindau-associated renal cell carcinoma. Mol Cell Biol 2005;25: 5675–86.
12. Carroll VA, Ashcroft M. Role of hypoxia-inducible factor (HIF)-1α versus HIF-2α in the regulation of HIF target genes in response to hypoxia, insulin-like growth factor-I, or loss of von Hippel-Lindau function: implications for targeting the HIF pathway. Cancer Res 2006;66:6264–70.
13. Dressler GR, Deutsch U, Chowdhury K, Nornes HO, Gruss P. Pax2, a new murine paired-box-containing gene and its expression in the developing excretory system. Development 1990;109: 787–95.
14. Ryan G, Steele-Perkins V, Morris JF, Rauscher FJ III, Dressler GR. Repression of Pax-2 by WT1 during normal kidney development. Development 1995;121:867–75.
15. Robson EJ, He SJ, Eccles MR. A PANorama of PAX genes in cancer and development. Nat Rev Cancer 2006;6:52–62.
16. Stayner CK, Cunliffe HE, Ward TA, Eccles MR. Cloning and characterization of the human PAX2 promoter. J Biol Chem 1998;273:25472–9.
17. Wu H, Chen Y, Liang J, et al. Hypomethylation-linked activation of PAX2 mediates tamoxifen-stimulated endometrial carcinogenesis. Nature 2005;438:981–7.
18. Memeo L, Jhang J, Assaad AM, et al. Immunohistochemical analysis for cytokeratin 7, KIT, and PAX2: value in the differential diagnosis of chromophobe cell carcinoma. Am J Clin Pathol 2007; 127:225–9.
19. Daniel L, Lechevallier E, Giorgi R, et al. Pax-2 expression in adult renal tumors. Hum Pathol 2001;32:282–7.
20. Mazal PR, Stichenwirth M, Koller A, Blach S, Haitel A, Susani M. Expression of aquaporins and PAX-2 compared to CD10 and cytokeratin 7 in renal neoplasms: a tissue microarray study. Mod Pathol 2004;18:535.
21. Hergovich A, Lisztwan J, Barry R, Ballschmieter P, Krek W. Regulation of microtubule stability by the von Hippel-Lindau tumour suppressor protein pVHL. Nat Cell Biol 2003;5:64–70.
22. Thoma CR, Frew IJ, Hoerner CR, Montani M, Moch H, Krek W. pVHL and GSK3β are components of a primary cilium-maintenance signalling network. Nat Cell Biol 2007;9: 588–95.
23. Kononen J, Bubendorf L, Kallioniemi A, et al. Tissue microarrays for high-throughput molecular

profiling of tumor specimens. Nat Med 1998;4:844–7.
24. Eble JN, Sauter G, Epstein JI, Sesterhenn IA. World Health Organization classification of tumours. Pathology and genetics of tumours of the male urinary system and male genital organs. IARC Press; 2004.
25. Rolfs A, Kvietikova I, Gassmann M, Wenger RH. Oxygen-regulated transferrin expression is mediated by hypoxia-inducible factor-1. J Biol Chem 1997;272:20055–62.
26. Arsham AM, Howell JJ, Simon MC. A novel hypoxia-inducible factor-independent hypoxic response regulating mammalian target of rapamycin and its targets. J Biol Chem 2003;278:29655–60.
27. Kominato Y, Iida R, Nakajima T, et al. Hypoxia induces upregulation of the deoxyribonuclease I gene in the human pancreatic cancer cell line QGP-1. Biochim Biophys Acta 2007;1770:1567–75.
28. Madan A, Curtin PT. A 24-base-pair sequence 3′ to the human erythropoietin gene contains a hypoxia-responsive transcriptional enhancer. Proc Natl Acad Sci U S A 1993;90:3928–32.
29. Schraml P, Struckmann K, Hatz F, et al. VHL mutations and their correlation with tumour cell proliferation, microvessel density, and patient prognosis in clear cell renal cell carcinoma. J Pathol 2002;196:186–93.
30. Gnarra JR, Dressler GR. Expression of Pax-2 in human renal cell carcinoma and growth inhibition by antisense oligonucleotides. Cancer Res 1995;55:4092–8.
31. Stuart ET, Haffner R, Oren M, Gruss P. Loss of p53 function through PAX-mediated transcriptional repression. EMBO J 1995;14:5638–45.
32. Stayner C, Iglesias DM, Goodyer PR, et al. Pax2 gene dosage influences cystogenesis in autosomal dominant polycystic kidney disease. Hum Mol Genet 2006;15:3520–8.
33. Winyard PJ, Risdon RA, Sams VR, Dressler GR, Woolf AS. The PAX2 transcription factor is expressed in cystic and hyperproliferative dysplastic epithelia in human kidney malformations. J Clin Invest 1996;98:451–9.
34. Ostrom L, Tang MJ, Gruss P, Dressler GR. Reduced Pax2 gene dosage increases apoptosis and slows the progression of renal cystic disease. Dev Biol 2000;219:250–8.
35. Schraml P, Frew IJ, Thoma CR, et al. Sporadic clear cell renal cell carcinoma but not the papillary type is characterized by severely reduced frequency of primary cilia. Mod Pathol 2008.
36. Solomon D, Schwartz A. Renal pathology in von Hippel-Lindau disease. Hum Pathol 1988;19:1072–9.
37. Choyke PL, Glenn GM, Walther MM, et al. The natural history of renal lesions in von Hippel-Lindau disease: a serial CT study in 28 patients. AJR Am J Roentgenol 1992;159:1229–34.
38. Dressler GR, Douglass EC. Pax-2 is a DNA-binding protein expressed in embryonic kidney and Wilms tumor. Proc Natl Acad Sci U S A 1992;89:1179–83.
39. Ordonez NG. The diagnostic utility of immunohistochemistry in distinguishing between mesothelioma and renal cell carcinoma: a comparative study. Hum Pathol 2004;35:697–710.
40. Campbell CE, Kuriyan NP, Rackley RR, et al. Constitutive expression of the Wilms tumor suppressor gene (WT1) in renal cell carcinoma. Int J Cancer 1998;78:182–8.
41. Niu Z, Ito M, Awakura Y, et al. The expression of NOV and WT1 in renal cell carcinoma: a quantitative reverse transcriptase-polymerase chain reaction analysis. J Urol 2005;174:1460–2.
42. Hueber PA, Waters P, Clark P, Eccles M, Goodyer P. PAX2 inactivation enhances cisplatin-induced apoptosis in renal carcinoma cells. Kidney Int 2006;69:1139–45.

Clinical Cancer Research

Loss of VHL and Hypoxia Provokes PAX2 Up-Regulation in Clear Cell Renal Cell Carcinoma

Van-Duc Luu, Gunther Boysen, Kirsten Struckmann, et al.

Clin Cancer Res 2009;15:3297-3304.